
Investigation of Suspension Characteristic and Development of Effective Suspension Model for Vehicle Roll Control



The University of Michigan-Dearborn
Henry W. Patton Center for Engineering
Education and Practice

Henry W. Patton Center for Engineering
Education and Practice
Annual Progress Report

Investigation of Suspension Characteristic and Development of Effective Suspension Model for Vehicle Roll Control

(Project #2006/9)

By:

Taehyun Shim
Associate Professor
Department of Mechanical Engineering

Table of Contents

Synopsis	iii
1. Background	1
2. Objectives	
3. Approach	
4. Results	
5. Conclusions.....	
6. Impact	
Educational	
Industrial	
7. Acknowledgments	
8. References.....	

Synopsis

In the development of active/passive roll control systems, a vehicle model that can represent realistic roll behavior is essential to predicting impending rollover as well as accurately applying the actuation force to avoid vehicle rollover. In this research, a low-order parametric vehicle model that produces a closed roll response is developed, and its response is compared to a multi-body-based vehicle model (or measured test data). To do this, a comprehensive algorithm that can reflect the effect of nonlinear suspension geometry on vehicle roll dynamics is designed. The low-order vehicle model incorporating a roll algorithm will be useful for both active and passive roll control system design.

1. Background

Rollover is recognized as one of the most important life-threatening factors in car accidents. According to statistics [1], nearly 33% of all deaths from passenger vehicle crashes result from rollovers. As sports utility vehicles (SUVs) are increasing on the road, rollover prevention systems or rollover warning systems are more important and have increasing demand from industries and drivers. However, predicting impending rollover is not simple.

To predict vehicle rollover from vehicle behavior, several types of vehicle rollover propensity systems have been introduced. For instance, as a static roll stability indicator, the static stability factor (SSF), which is a ratio of the half track width to the height of vehicle's center of gravity, is commonly used to predict vehicle rollover [2]. This factor is used as a threshold for predicting rollover. If the lateral acceleration exceeds the threshold, vehicle rollover is imminent. However, since it is obtained under the assumption that a vehicle is a rigid body, this factor is too conservative, and thus vehicle rollover often occurs even when the lateral acceleration is less than the factor. Some modifications for the static indicator have been introduced by using more complex vehicle roll models that include the effects of suspension or tire compliance [3–5]. However, these indicators only use static thresholds in terms of the lateral acceleration in order to decide whether vehicle rollover is imminent or not.

To provide more realistic rollover warning, dynamic approaches have been suggested, such as the time-to-rollover (TTR) metric [6], the lateral load transfer ratio (LTR) [7, 8], the dynamic stability index (DSI) [9], and the critical energy-based measure [10, 11]. For example, the TTR metric measures the time to reach the critical roll angle. The DSI, which is a function of the lateral acceleration and the roll acceleration of the sprung mass, determines vehicle rollover whenever the DSI exceeds the SSF. The critical energy-based rollover threat indicator is defined as the point of lowest potential energy, which happens at the critical point of two-wheel lift-off. In this algorithm, a vehicle is on a critical condition when the value of the indicator is less than zero. However, the aforementioned algorithms do not consider the importance of the location of the roll center in predicting rollover. The roll center in vehicle rolling motion is an important parameter. That is, the roll center moves laterally and vertically due to asymmetric suspension geometry while a vehicle rolls, and could affect roll responses and further rollover warning systems.

In the development of active/passive roll control systems, the vehicle model that can represent realistic roll behavior is essential to predicting impending rollover as well as accurately applying the actuation force to avoid vehicle rollover. A number of vehicle models have been introduced in the literature for application of active/passive roll control systems. These models are typically low-order roll plane models with one-dimensional suspensions, and derived from various assumptions and limitations. Thus, it is difficult to know the validity of these outside of the specific application. Often these models show a considerable discrepancy compared to measured data when its responses are compared to the region in which vehicle dynamics is dictated by nonlinear characteristics of the suspension and tires. In vehicle roll dynamics, for instance, the effect of roll center movement becomes important as a vehicle roll angle grows. This results in a jacking force, which is one of the major factors causing a vehicle rollover. Since

the roll center is assumed as a fixed point during the roll motion in most vehicle models cited in the literature [6, 12–15], these models cannot predict the jacking force effect. Although a multi-body-based vehicle model can reveal these phenomena, it is difficult to use these models in the prediction and control algorithm due to computational time. Thus it is desirable to develop a low-order vehicle model that can reveal these effects.

2. Objectives

The overall objective of this research is to develop a low-order parametric vehicle model that produces a closed roll response, which is compared to a multi-body-based vehicle model (or measured test data). A comprehensive algorithm that can reflect the effect of nonlinear suspension geometry on vehicle roll dynamics will be developed. The low-order vehicle model incorporating a roll algorithm will be useful for both active and passive roll control system design.

3. Approach

This project will first develop multi-body vehicle models with a combination of different types of suspensions. Once multi-body vehicle models are developed, a comprehensive study of the roll behavior of these models is assessed by performing vehicle maneuvers such as J-turns and fishhooks. The roll sensitivity analysis for the factors ignored in the roll plane model is evaluated, and its responses are compared with those of a low-order parametric vehicle model with 1-D and 2-D suspensions. A comprehensive algorithm that improves the roll response of the low-order model is then developed using measurable vehicle outputs.

4. Results

4.1 The concept of roll compensation at a low-order vehicle model

This section deals with the compensation for the roll response of a low-order vehicle model equipped with simple 1-D suspension by injecting an additional roll moment into roll dynamics. The additional roll moment is calculated from roll center locations and nonlinear suspension characteristics.

The roll center, which is defined as a point at which lateral forces applied to the sprung mass do not produce suspension roll [16, 17], is a fictitious parameter that can quantify the effects of suspension geometry on the roll angle. As a vehicle rolls, the roll center moves laterally and vertically due to the asymmetric suspension geometry.

The schematic of the roll center estimation algorithm is shown in Figure 1. Consider a low-order vehicle model that has a fixed roll center. The low-order model generates roll motions that include no effect of the roll center movement, where the model is driven by the lateral acceleration obtained from a full vehicle model, including the effect of the roll center movement. As an actual vehicle model, a full vehicle model is considered. It could be an actual vehicle, an Adams vehicle model, or a CarSim vehicle model. The full vehicle model includes nonlinear suspension geometry, and thus can realize the effect of roll center movement and produce realistic rolling behavior and lateral motion.

The strategy of roll compensation is as follows: first, actual roll motions, including roll angle and roll rate ($\phi_m, \dot{\phi}_m$), is obtained from, for example, a CarSim model, which includes nonlinear suspension models, by a driver's inputs. Second, the lateral acceleration from a CarSim model drives a simple low-order vehicle model, where it is assumed that the location of vehicle roll center is fixed. Through the low-order model, roll angle and roll rate ($\phi_f, \dot{\phi}_f$) are obtained. Then, the errors of the roll angle and the roll rate between the two models are used to estimate the effective roll stiffness, effective roll damping, and lateral and vertical roll center movement utilizing a parameter identification algorithm. Finally, an additional roll moment, which is a function of the estimated parameters, is calculated and injected into the low-order vehicle model.

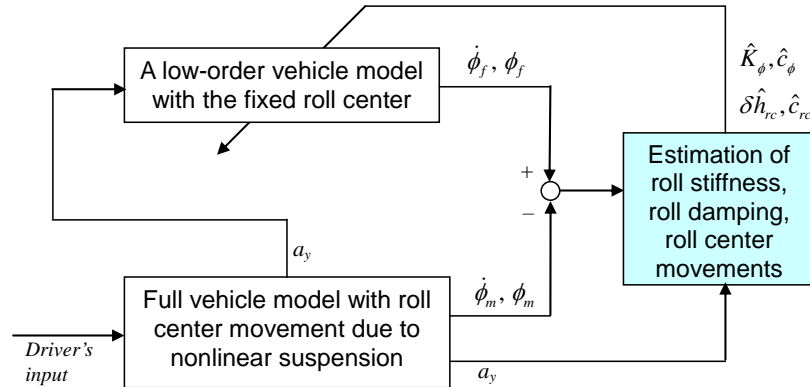
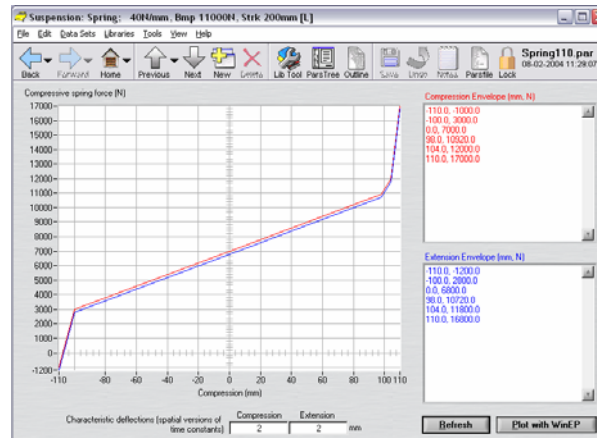
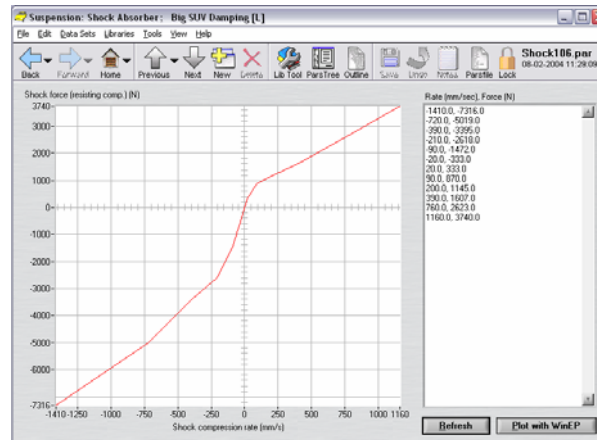


Figure 1. The schematic diagram of roll compensation.

This work selects a CarSim model as a full vehicle model. This model includes the property of asymmetric suspension geometry. A type of independent suspension system and a type of a solid axle system are chosen as front and rear suspensions, respectively. In the front and rear parts, the suspensions have nonlinear properties in suspension stiffness and damping, as shown in Figure 2. In this nonlinear suspension model, the suspension stiffness rapidly increases as a suspension stroke crosses a linear range. The suspension damping has the characteristics of a nonlinear curve, as shown in Figure 2. These nonlinear suspension characteristics result in jacking forces during roll motion, which forces the location of the roll center to move laterally and vertically.



(a) Nonlinear suspension stiffness



(b) Nonlinear suspension damping

Figure 2. Nonlinear suspension characteristics in the front axle.

4.2 Parameter estimation algorithm for the roll compensation

This section introduces a strategy of identifying unknown parameters, which is used to calculate the compensation roll moment. The parameters are the effective roll stiffness, effective roll damping, lateral roll center movement, and vertical roll center movement.

Consider a roll plane model including the roll center as shown in Figure 3, where the vehicle body rolls along the roll center. In detail, this model has a roll degree of freedom for the suspension that connects the sprung mass and unsprung masses, and its sprung mass is assumed to rotate at a roll center. The roll center is usually modeled in a roll plane model as it is located on the centerline of the sprung mass. However, the roll center is moved horizontally and vertically as the body rolls. This model assumes that the roll center is not fixed. Thus the sprung mass rotates at a point denoted as rc in Figure 3, which is defined a moving roll center. The parameters h_{rc} and c_{rc} in Figure 3 denote the height and the lateral offset of the roll center, respectively. In the case of the fixed roll center model, the height of the roll center h_{rc} is set to be fixed and the length of the lateral movement c_{rc} is set to be zero, respectively.

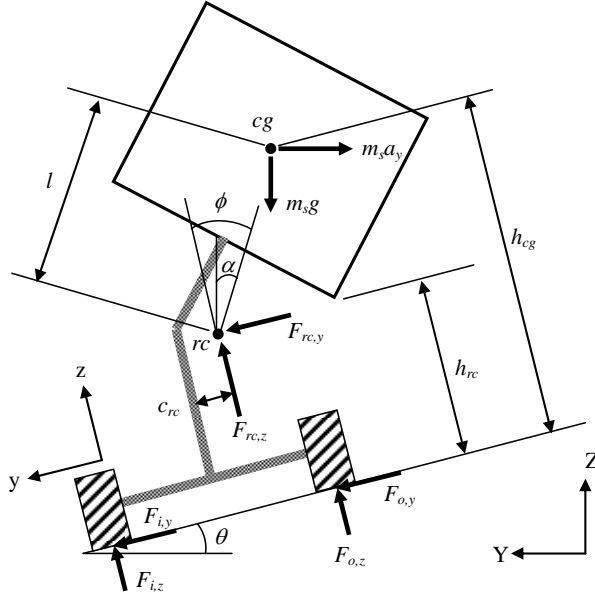


Figure 3. A suspended roll model including roll center movement.

Consider roll dynamics in terms of the effective suspension roll stiffness and roll damping for the low-order vehicle model, which is derived from the moment balance at the roll center in Figure 3, when the roll center is located on the centerline of the sprung mass, i.e., $c_{rc} = 0$, and the road bank angle is zero. Here it is assumed that the height of the roll center is fixed. The simple roll dynamics are expressed as

$$c_{\phi}^f \dot{\phi}_f + K_{\phi}^f \phi_f = m_s a_y (h_{cg} - h_{rc}^f) + m_s g (h_{cg} - h_{rc}^f) \tan \phi_f \quad (1)$$

where suspension parameters c_{ϕ}^f and K_{ϕ}^f are constant and assumed to be known, and the fixed roll center height and the height of the center of gravity from ground are assumed to be known. This dynamic is driven by lateral acceleration, which is fairly precise since the lateral acceleration is generated from a full vehicle model. The roll dynamics in this model can be simplified as

$$c_{\phi}^m \dot{\phi}_m + K_{\phi}^m \phi_m = m_s a_y (h_{cg} - h_{rc}) + m_s g (h_{cg} - h_{rc}) \tan \phi_m \quad (2)$$

where $h_{rc} := h_{rc}^f + \delta_{hrc}$ and δ_{hrc} is the vertical movement of the roll center. The vertical movement δ_{hrc} varies as a vehicle rolls. Subtracting (2) from (1) yields

$$c_{\phi}^f (\dot{\phi}_f - \dot{\phi}_m) + K_{\phi}^f (\phi_f - \phi_m) = m_s a_y \delta_{hrc} + m_s g (h_{cg} - h_{rc}^f) \tan \phi_f - m_s g (h_{cg} - h_{rc}^f - \delta_{hrc}) \tan \phi_m + \Delta K_{\phi} \phi_m + \Delta c_{\phi} \dot{\phi}_m \quad (3)$$

where $\Delta c_{\phi} := c_{\phi}^m - c_{\phi}^f$ and $\Delta K_{\phi} := K_{\phi}^m - K_{\phi}^f$ are defined as deviations from the nominal values for the suspension parameters. By assuming $(\tan \phi_f - \tan \phi_m) \approx (\phi_f - \phi_m)$, the error dynamics between the two roll dynamics in (3) can be expressed as

$$c_{\phi}^f (\dot{\phi}_f - \dot{\phi}_m) + (K_{\phi}^f - m_s g (h_{cg} - h_{rc}^f)) (\phi_f - \phi_m) = (m_s a_y + m_s g \tan \phi_m) \delta_{hrc} + \Delta K_{\phi} \phi_m + \Delta c_{\phi} \dot{\phi}_m \quad (4)$$

where δh_{rc} , ΔK_ϕ and Δc_ϕ are unknown parameters. The above equation is written to the regression model as follows:

$$Y = \Phi^T \Theta \quad (5)$$

where

$$Y = c_\phi^f (\dot{\phi}_f - \dot{\phi}_m) + (K_\phi^f - m_s g (h_{cg} - h_{rc}^f)) (\phi_f - \phi_m)$$

$$\Phi = \begin{bmatrix} m_s a_y + m_s g \tan \phi_m & \phi_m & \dot{\phi}_m \end{bmatrix}^T$$

$$\Theta = \begin{bmatrix} \delta h_{rc} \\ \Delta K_\phi \\ \Delta c_\phi \end{bmatrix}.$$

Here the parameter vector Θ will be estimated.

In addition, by comparing the geometry between the fixed roll center model and the moving roll center model, as shown in Figure 3, the lateral movement of the roll center can be approximated as

$$\begin{aligned} c_{rc} &\approx (h_{cg} - h_{rc}^f) \tan \phi_f - (h_{cg} - h_{rc}) \tan \phi_m \\ &= (h_{cg} - h_{rc}^f) (\tan \phi_f - \tan \phi_m) + \delta h_{rc} \tan \phi_m \\ &\approx (h_{cg} - h_{rc}^f) (\phi_f - \phi_m) + \delta h_{rc} \tan \phi_m \end{aligned} \quad (6)$$

where the vertical roll center deviation is used to obtain the lateral roll center deviation. A parameter estimation algorithm such as the standard recursive least square (RLS) method can be used to estimate these roll center movements.

By comparing (1) and (3), the additional roll moment for the compensation can be calculated as a function of the estimated roll stiffness, estimated roll damping, estimated lateral roll center movement, and the estimated vertical roll center movement as follows:

$$M_{x,additional} = -m_s a_y \hat{\delta}_{hrc} - m_s g \hat{c}_{rc} - \Delta \hat{K}_\phi \phi_m - \Delta \hat{c}_\phi \dot{\phi}_m \quad (7)$$

where $\hat{\delta}_{hrc}$, \hat{c}_{rc} , $\Delta \hat{K}_\phi$, and $\Delta \hat{c}_\phi$ are the estimated parameters using the following parameter estimation algorithm.

A RLS scheme with multiple forgetting is effective in identifying unknown parameters that are time-varying with different rates. Using single forgetting is difficult in RLS. In the standard method it is assumed that parameters vary with similar rates. Thus, the errors from all parameters are lumped into a single term. This structure cannot realize if the error is due to one or more parameters. However, using multiple forgetting, one can separate the error due to each parameter. The detailed algorithm for identifying three parameters with different rates is as follows [18]:

$$\begin{bmatrix} \hat{\theta}_1(k) \\ \hat{\theta}_2(k) \\ \hat{\theta}_3(k) \end{bmatrix} = \begin{bmatrix} 1 & L_1(k)\phi_2(k) & L_1(k)\phi_3(k) \\ L_2(k)\phi_1(k) & 1 & L_2(k)\phi_3(k) \\ L_3(k)\phi_1(k) & L_3(k)\phi_2(k) & 1 \end{bmatrix}^{-1} \begin{bmatrix} \hat{\theta}_1(k-1) + L_1(k)(y(k) - \phi_1(k)\hat{\theta}_1(k-1)) \\ \hat{\theta}_2(k-1) + L_2(k)(y(k) - \phi_2(k)\hat{\theta}_2(k-1)) \\ \hat{\theta}_3(k-1) + L_3(k)(y(k) - \phi_3(k)\hat{\theta}_3(k-1)) \end{bmatrix} \quad (8)$$

where

$$L_1(k) = P_1(k-1)\phi_1(k)\left(\lambda_1 + \phi_1^T(k)P_1(k-1)\phi_1(k)\right)^{-1}$$

$$P_1(k) = \left(I - L_1(k)\phi_1^T(k)\right)P_1(k-1)\frac{1}{\lambda_1}$$

$$L_2(k) = P_2(k-1)\phi_2(k)\left(\lambda_2 + \phi_2^T(k)P_2(k-1)\phi_2(k)\right)^{-1}$$

$$P_2(k) = \left(I - L_2(k)\phi_2^T(k)\right)P_2(k-1)\frac{1}{\lambda_2}$$

$$L_3(k) = P_3(k-1)\phi_3(k)\left(\lambda_3 + \phi_3^T(k)P_3(k-1)\phi_3(k)\right)^{-1}$$

$$P_3(k) = \left(I - L_3(k)\phi_3^T(k)\right)P_3(k-1)\frac{1}{\lambda_3}$$

Here λ_1 , λ_2 , and λ_3 denote multiple forgetting factors for each parameter, respectively. The forgetting factors are selected by inspecting the time varying rates.

4.3. Application: Roll stability indicator incorporating the estimated parameters

The estimated parameters can be also applied to develop a roll stability indicator for roll stability controllers, where the estimated parameters described in Section 4.3 are used to calculate the level of the roll stability indicator. The detailed derivation of the roll stability indicator can be found in [4].

The roll stability indicator can be derived from the force and moment equations in the suspended roll model. The summation of forces for the sprung mass in the Y- and Z-directions is calculated as

$$\sum F_Y = F_{rc,y} \cos \theta + F_{rc,z} \sin \theta - m_s a_y = 0 \quad (9)$$

$$\sum F_Z = -F_{rc,y} \sin \theta + F_{rc,z} \cos \theta - m_s g = 0 \quad (10)$$

where $F_{rc,y}$ and $F_{rc,z}$ denote reaction forces at the roll center, θ and m_s are the road bank angle and the sprung mass, and a_y represents the lateral acceleration. Summing moments about the roll center for the sprung mass and about the outer tire contact point yield

$$\sum M_{rc} = m_s a_y l \cos \alpha + m_s g l \sin \alpha - K_\phi \phi = 0 \quad (11)$$

$$\sum M_o = K_\phi \phi + F_{rc,y} h_{rc} - F_{rc,z} (t/2 - c_{rc}) + F_{i,z} t = 0 \quad (12)$$

where l , t , K_ϕ and ϕ denote the distance between the center of gravity and the roll center, the track width, the roll stiffness, and the body roll angle, respectively. The roll center parameters h_{rc} and c_{rc} are assumed to change as the vehicle rolls. The roll center reaction forces, after manipulating (9) and (10), are found to be

$$F_{rc,y} = m_s a_y \cos \theta - m_s g \sin \theta \quad (13)$$

$$F_{rc,z} = m_s g \cos \theta + m_s a_y \sin \theta \quad (14)$$

Using the geometry of the moment arm in Figure 3, described by

$$l \cos \phi = h_{cg} - h_{rc} \quad (15)$$

and the moment equation of (11), the following equation is calculated:

$$\begin{aligned} K_\phi \phi &= m_s a_y l \cos(\phi - \theta) + m_s g l \sin(\phi - \theta) \\ &= m_s (h_{cg,s} - h_{rc}) \cdot (a_y \cos \theta - g \sin \theta + (a_y \sin \theta + g \cos \theta) \tan \phi) \end{aligned} \quad (16)$$

Substituting the roll center reaction forces of (13) and (14) into (4), and letting $F_{iz} = 0$, this becomes

$$K_\phi \phi + m_s (a_y^\phi \cos \theta - g \sin \theta) h_{rc} - m_s (a_y^\phi \sin \theta + g \cos \theta) (t/2 - c_{rc}) = 0 \quad (17)$$

By substituting (16) into (17), the above equation yields

$$\left(\frac{a_y^\phi}{g} \cos \theta - \sin \theta \right) h_{cg} = \left(\frac{a_y^\phi}{g} \sin \theta + \cos \theta \right) \cdot \left((t/2 - c_{rc}) - (h_{cg,s} - h_{rc}) \tan \phi \right) \quad (18)$$

By furthermore manipulating and solving for a_y^ϕ , the roll stability indicator becomes

$$\frac{a_y^\phi}{g} = \frac{e + \frac{t^*}{2h^*}}{1 - e \frac{t^*}{2h^*}} \quad (19)$$

with

$$e = \tan \theta$$

$$t^* = t - 2c_{rc} - 2(h_{cg} - h_{rc}) \tan \phi$$

$$h^* = h_{cg}$$

where the parameters e , t^* , and h^* are defined as the modified superelevation, modified track width, and the modified center of gravity height, respectively.

Equation (19) implies that the roll stability indicator depends on the location of the roll center, the height of the vehicle's center of gravity, and the roll angle. This indicator is a dynamic one in the sense that it changes dynamically as a vehicle rolls. The level of the indicator can determine whether a vehicle rolls over or not. If the level of the lateral acceleration is larger than that of the indicator, vehicle rollover is imminent. In order to determine the exact value of the indicator, the roll center movement should be calculated or estimated from other vehicle outputs.

In this work, the roll stability indicator of (19) is rewritten to include the estimated parameters of the roll center movements as follows:

$$\frac{a_y^\phi}{g} = \frac{e + \frac{\hat{t}^*}{2h^*}}{1 - e \frac{\hat{t}^*}{2h^*}} \quad (20)$$

with

$$e = \tan \theta$$

$$\hat{t}^* = t - 2\hat{c}_{rc} - 2(h_{cg} - h_{rc} - \hat{\delta}_{hrc}) \tan \phi$$

$$h^* = h_{cg}$$

where \hat{c}_{rc} and $\hat{\delta}_{hrc}$ denote the estimated parameters of c_{rc} and δ_{hrc} , respectively. Equation (20) means that the roll center movement information is incorporated to determine the roll center indicator.

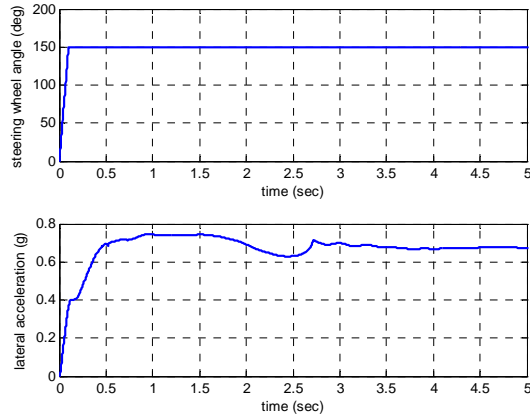
4.4 Simulation

In this section, the parameter estimation algorithm is evaluated and the effectiveness of the compensation of the roll motion is demonstrated through simulations.

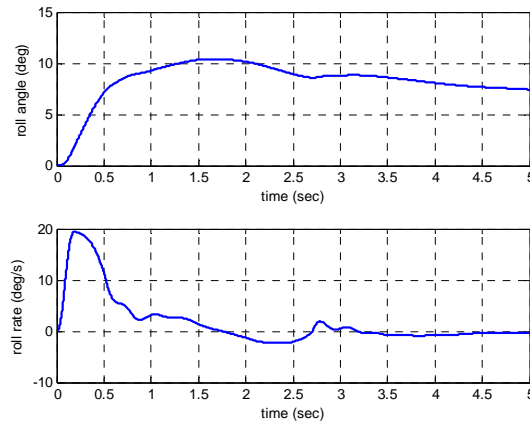
The vehicle motion of the full vehicle model shown in Figure 1 is generated from a CarSim model. Here, a big SUV model with the nonlinear suspension stiffness and damping shown in Figure 2 is selected as the full car model. The vehicle parameters are as follows: a center of gravity height of 900 mm, the sprung mass of 2210 kg, initial front roll center height of 230 mm, initial rear roll center height of 350 mm, and track width of 1600 mm.

Some scenarios are conducted in the cases of J-turn maneuvers and a fishhook maneuver. First, two scenarios of the J-turn maneuver are conducted with different initial forward speeds: one is for a non-rollover incident and the other is for a rollover incident. Second, a fishhook maneuver is conducted at a low initial velocity as a non-rollover case.

For the first non-rollover case, the steering wheel angle and the initial speed are set to be 150 °and 100 km/h, respectively. The lateral acceleration and roll behavior in this case are illustrated in Figure 4. As shown in this figure, the lateral acceleration remains within 0.8 g, the roll angle keeps within 11°, and the roll rate converges to zero, which is a normal driving condition that does not induce vehicle rollover.



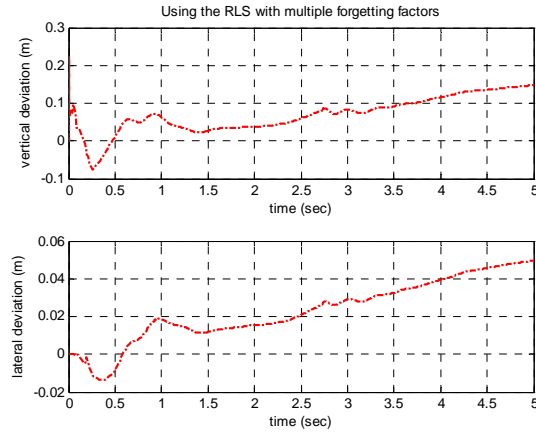
(a) Steering wheel angle and lateral acceleration



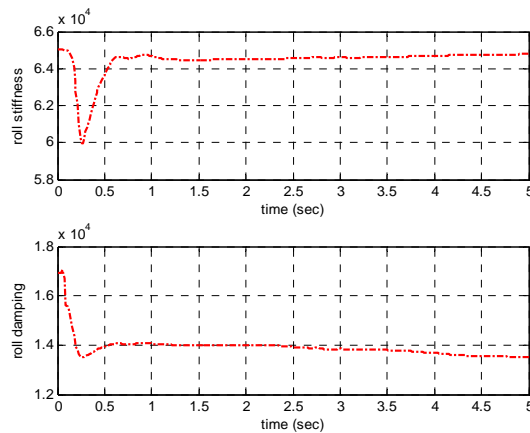
(b) Roll angle and roll rate

Figure 4. Steering input and vehicle outputs (J-turn 150°, 100 km/h).

Using RLS with multiple forgetting, the unknown parameters, which are the effective roll stiffness, effective roll damping coefficient, lateral roll center movement, and the vertical roll center movement, are estimated as shown in Figure 5. These estimated parameters will be used to calculate the additional roll moment to compensate for the roll response in a low-order vehicle model with a fixed roll center.



(a) Estimated roll center movement



(b) Estimated roll stiffness and roll damping

Figure 5. Estimated roll center movement and suspension characteristics (J-turn 150°, 100 km/h).

The effectiveness of the compensation is demonstrated in Figure 6, where *fixed model*, *CarSim*, and *fixed rc model with the compensation* denote the output from a simple low-order vehicle model with its fixed roll center, the output from a CarSim model, and the output from the low-order vehicle model by injecting the additional roll moment, respectively. As shown in this figure, the result of the compensation by injecting the additional roll moment into the low-order vehicle model with the fixed roll center works fairly well in transient as well as steady state. That is, just by adding the additional roll moment in terms of the effective roll stiffness and damping and the roll center movement, the roll behavior of a simple roll model can be close to that of the CarSim model. This implies that compensating the effect of roll center movement into a simple roll model can describe a realistic roll motion that can be obtained from a full vehicle model or real data.

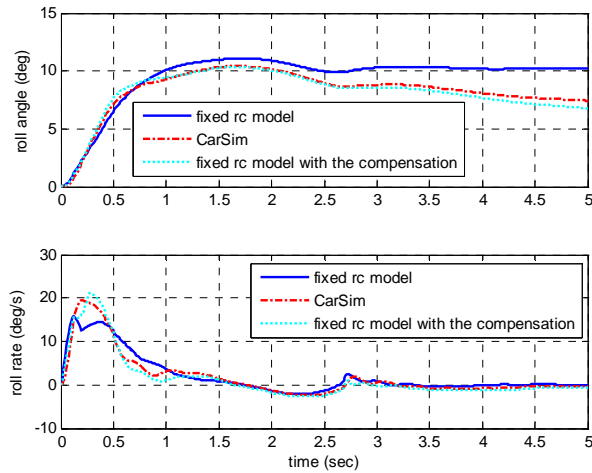
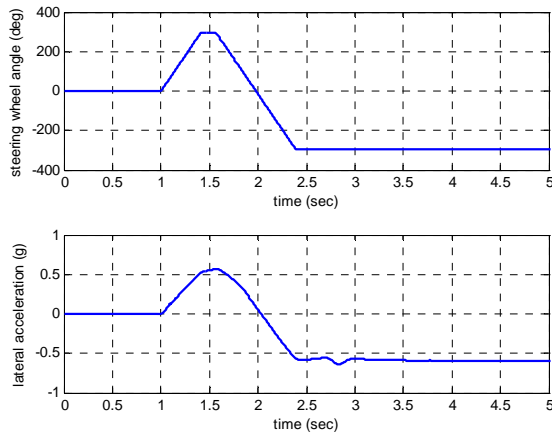
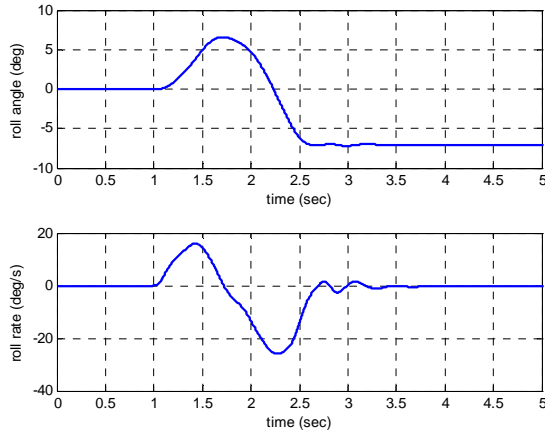


Figure 6. Compensation of the roll angle and roll rate.

For the second non-rollover case, a fishhook maneuver is conducted at a low initial speed of 35 km/h. The steering wheel angle, lateral acceleration, roll angle, and the roll rate are illustrated in Figure 7. As shown in Figure 7, the lateral acceleration remains within 0.6 g, and the roll angle stays within 7°, which means that a vehicle rollover does not occur.



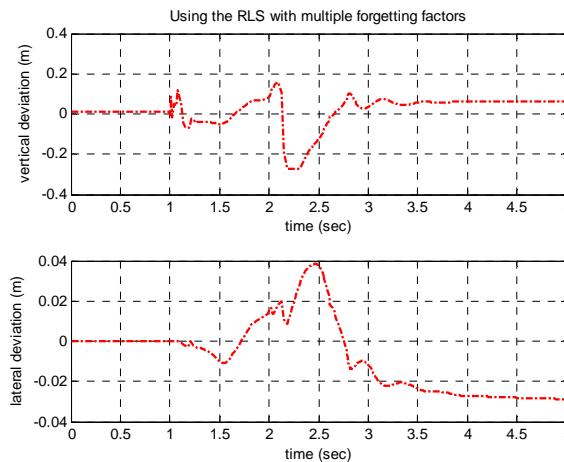
(a) Steering wheel angle and lateral acceleration



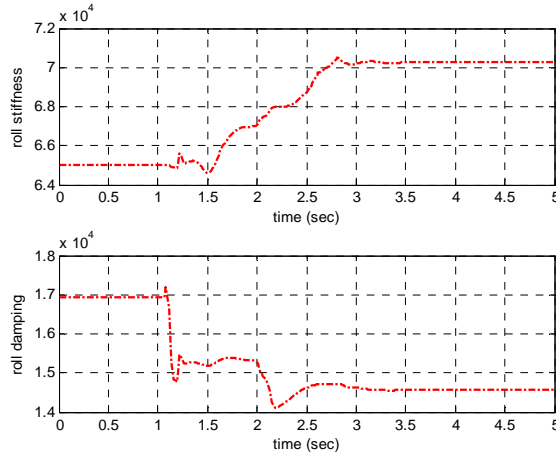
(b) Roll angle and roll rate

Figure 7. Vehicle input and outputs (fishhook maneuver).

Figure 8 illustrates the estimated parameters, where the effective roll stiffness, effective roll damping, lateral roll center movement, and the vertical roll center movement are estimated. As shown in this figure, the estimated parameters are quite reasonable. In the vertical movement of the roll center, the steady-state value is increased from the initial one, because the suspension operates in a nonlinear region. When the suspension hits the bump stop, the value of the spring stiffness rapidly increases. This phenomenon results in increased effective roll stiffness. In the lateral movement of the roll center, as a vehicle roll changes from positive to negative values, the lateral movement is changes from positive to negative. And in the suspension characteristics, when the suspension operates in a nonlinear region, the effective roll stiffness increases and the effective roll damping coefficient decreases. This increase and decrease are hypothesized from the suspension characteristics shown in Figure 2. Using these estimated parameters, the roll responses in a low-order vehicle model can be compensated.



(a) Estimated roll center movement



(b) Estimated roll stiffness and roll damping

Figure 8. Estimation of roll center movement and suspension characteristics (fishhook maneuver).

Figure 9 shows the effectiveness of the proposed roll compensation strategy. As shown in this figure, the result of the compensation by injecting the additional roll moment into the low-order vehicle model with a fixed roll center warns fairly well in transient as well as steady state. That is, by just adding the additional roll moment in terms of the suspension characteristics and the location of the roll center, the roll behavior of a simple roll model can be close to that of the CarSim model.

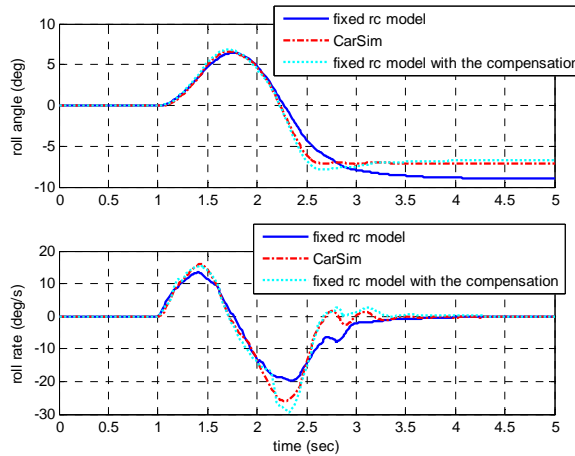
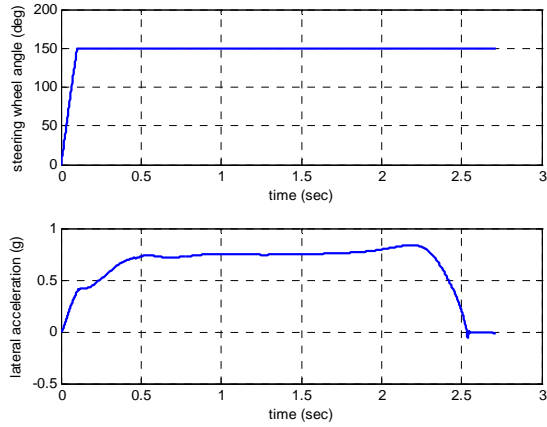
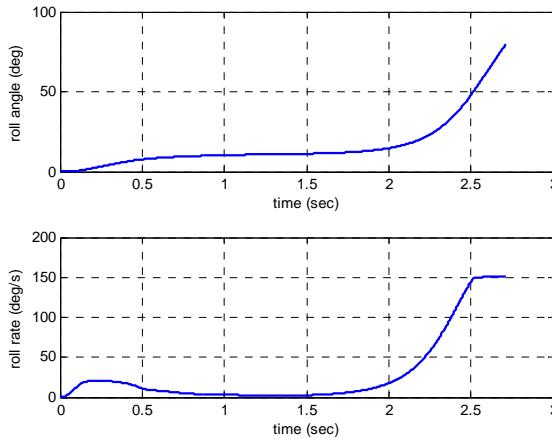


Figure 9. Compensated roll angle and roll rate (fishhook maneuver).

For a rollover case, a J-turn maneuver is conducted with a high initial speed of 130 km/h. Figure 10 shows the vehicle input and outputs, where the lateral acceleration, roll angle, and the roll rate are illustrated when the steering wheel angle reaches a maximum of 150° . As shown in this figure, the roll angle and the roll rate increase, and as a result, the vehicle rolls over.



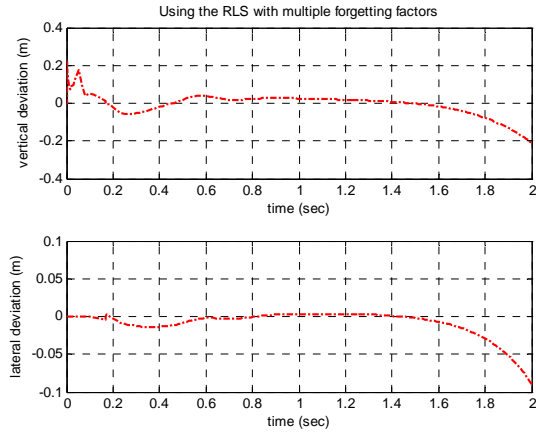
(a) Steering wheel angle and lateral acceleration



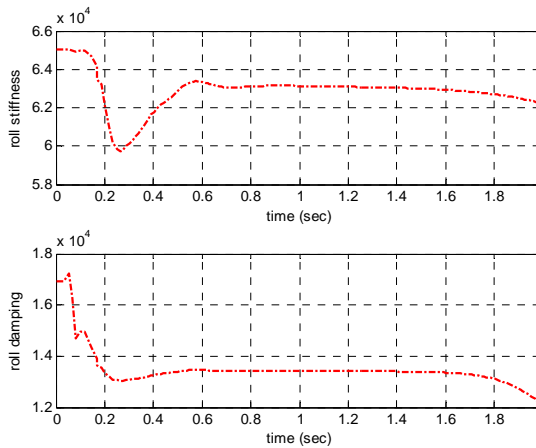
(b) Roll angle and roll rate

Figure 10. Steering input and vehicle outputs.

Figure 11 illustrates the estimation results of the parameters, where the effective roll stiffness, effective roll damping coefficient, lateral roll center movement, and the vertical roll center movement are estimated, respectively. These estimated values will be used to generate the additional roll moment.



(a) Estimated roll center movement



(b) Estimated roll stiffness and roll damping

Figure 11. Estimation of roll center movement and suspension characteristics.

In Figure 12, the result of the compensation is illustrated by injecting the additional roll moment into the low-order vehicle model with a fixed roll center. As shown in this figure, the compensation works quite well even when the roll angle and the roll rate increase, or as a vehicle rollover is impending. Using the low-order vehicle model with the fixed roll center, the lateral acceleration shown in Figure 10 does not drive the vehicle rollover. Using the same lateral acceleration in a CarSim model, the vehicle roll angle and the roll rate increase, and finally a vehicle rolls over. However, by injecting the additional roll moment into the low-order vehicle model, vehicle rollover is realized.

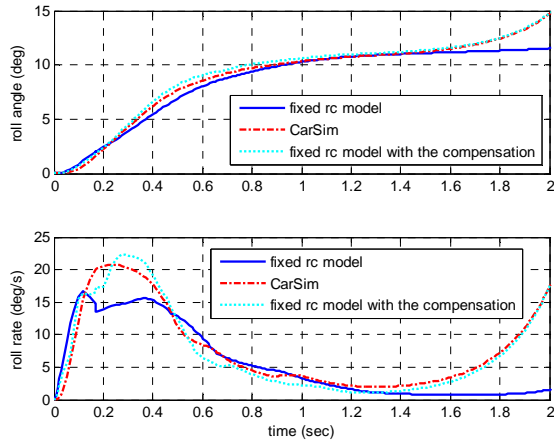


Figure 12. Compensation of roll angle and roll rate.

As another application of parameter estimation, a roll stability indicator is introduced in Section 4.3. As mentioned before, the estimated roll center movements are used to determine the roll stability indicator. From here, the performance of the proposed indicator is demonstrated. Figure 13 shows the roll stability boundary for the proposed roll stability indicator, where the vehicle motion crosses over the boundary. It means that two wheels lift off from the ground and a vehicle rolls over. The SSF denotes the static stability factor, which is calculated as a ratio of the half track width to the height of vehicle’s center of gravity. The SSF value is commonly used to warn the driver of vehicle rollover. As shown in this figure, the vehicle motion does not cross the SSF line, which means that a vehicle rollover does not occur. However, as shown in Figure 10, the vehicle rolls over. It means that using the SSF to indicate rollover gives limitations and thus the SSF may not be used as a suitable rollover warning device, while the proposed roll stability index indicates vehicle rollover correctly, as shown in Figure 13.

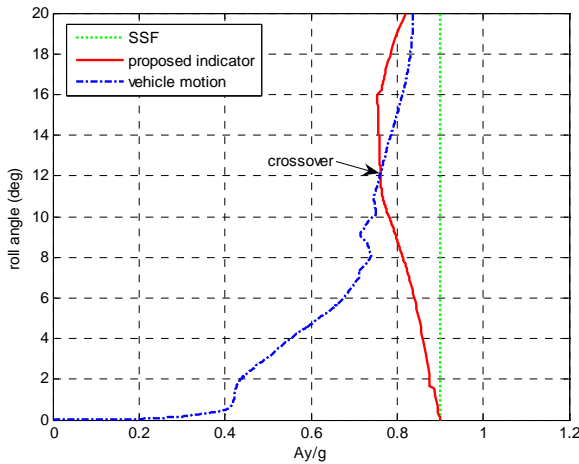


Figure 13. The proposed roll stability indicator.

In addition, the performance of the indicator is compared with the existing rollover propensities such as the load transfer ratio (LTR), energy-based measure, and the dynamic stability index (DSI). The detailed description for each indicator is as follows.

The LTR is defined as [8]:

$$LTR := \frac{F_{zr} - F_{zl}}{F_{zr} + F_{zl}}$$

where F_{zr} and F_{zl} denote the total vertical load at the right and left wheels, respectively. The value of LTR varies from 0 for runs with no lateral load transfer to 1 when two wheels lift off. The DSI is defined as the sum of the lateral acceleration and the roll acceleration as follows [9]:

$$DSI := \frac{a_y}{g} + \frac{I_{xxs}\alpha}{mgh_{cg}}$$

where α is the sprung mass roll acceleration and I_{xxs} is the sprung mass roll moment of inertia. Vehicle rollover will occur when the DSI exceeds the SSF. The W_{WLO} , which is energy-based measure, is the local maximum point of potential energy and is calculated as follows [11]:

$$W_{WLO} := \frac{E_{crit} - E_{roll}}{E_{crit}}$$

where E_{roll} and E_{crit} denote the total energy in the roll moment and the total energy at the critical situation, respectively. The total energy E_{roll} is calculated from the sum of the potential and kinetic energy. The critical energy E_{crit} is obtained from E_{roll} when two wheels lift off.

The performance of the indicators is compared in Table I, where warning time denotes the indicated time to rollover from each indicator. The roll angle and the roll rate at that time are compared. The proposed indicator warns of rollover at 1.75 sec, which is slower than LTR but faster than W_{WLO} and DSI. From the two indicators of W_{WLO} and DSI, the roll angles and roll rates are too large, which means that these seem to be close to realistic rollover time, but it is impossible or hard to control or prevent rollover by actuators in these situations. Also, in the case of LTR that indicates a two-wheel liftoff time, it might be too early for detection of rollover.

Table I. Comparison of the rollover warning indices.

Rollover indices	Indicated time (sec)	Roll angle (deg)	Roll rate (deg/s)
LTR	0.67	9.1	6.9
Proposed	1.75	12.1	5.9
DSI	2.04	15.5	21
WLO	2.12	17.5	30.9
SSF	NOT	-	-

The phase plane of the roll angle and the roll rate is shown in Figure 14, where the rollover warning times by each indicator are compared. First, LTR gives a warning signal, followed by the proposed one, then DSI and W_{WLO} as the roll angle increases. The simulation results imply that the proposed roll stability indicator incorporating the roll center movement can be potentially used to predict impending rollover for rollover prevention systems.

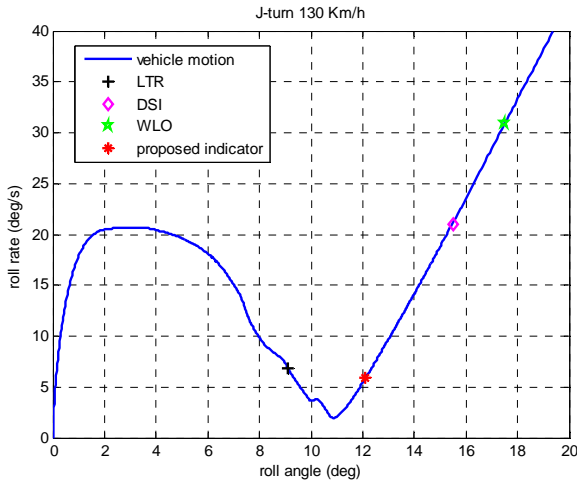


Figure 14 Phase plane between the roll angle and the roll rate

In summary, in this work, a compensation strategy for the roll motion in a low-order vehicle model is proposed. The compensation is conducted by generating the additional roll moment, which is a function of the effective roll stiffness, the effective roll damping coefficient, and the roll center movement. In order to estimate the vehicle parameters, a recursive least square scheme with multiple forgetting factors is applied. The simulation results show that the compensated roll motion is close to that of a CarSim model.

In addition, as another application of the vehicle parameter estimation, a dynamic roll stability indicator is proposed by incorporating roll center movement, where the estimated horizontal and vertical roll center migrations are used to calculate the value. The simulation results show that the stability indicator gives better performance and provides earlier detection for rollover than some of the existing dynamic roll stability indices. It could be potentially used to predict impending vehicle rollover.

5. Conclusions

A vehicle model with simple 1-D suspension with equivalent spring stiffness and damping is widely used in the development of vehicle control systems. The proposed work is only focused on the improvement of vehicle roll responses (roll angle, roll rate, etc.) in 1-D suspension by including the effects of roll center movement and jacking forces since it is very difficult to match all aspects of vehicle responses to one with simplified suspension and the other with definite suspension geometry. As shown

in the previous result, the proposed algorithm shows promising results to estimate the roll center movement of actual vehicle.

6. Impact

Educational:

The PI is responsible for three graduate courses: AE 502 Modeling of Automotive Systems, ME 543 Vehicle Dynamics, and AE 555 Vehicle Stability and Control. The low-order vehicle model and the nonlinear suspension effects on vehicle roll responses investigated in this project will be of great value for these courses. The effects of suspension design on vehicle roll and handling responses can also be incorporated. Homework and a project-related topic will enhance the understanding of vehicle handling and rollover resistance.

Industrial:

Although active and passive roll control systems exist to prevent vehicle rollover, a great deal still remains to be done to improve their effectiveness. The knowledge gained here can be useful for the roll control algorithm, including detection of wheel liftoff, assessment of transient roll behavior, and model-based active roll control system development.

7. Acknowledgments

We would like to thank our sponsors, Drs. Davor Hrovat and Jahan Asgari from the Ford Motor Company, for their encouragement and assistance in providing valuable suggestions. We would also like to thank the Henry W. Patton Center for Engineering Education and Practice at the University of Michigan-Dearborn for the financial support of this project.

8. References

- [1] National Highway Traffic Safety Administration. <<http://www.nhtsa.dot.gov/cars/testing/ncap/rollover/pages/RolloCharFat.htm>>.
- [2] Christos, J.P. and D.A. Guenther. "The Measurement of Static Rollover Metrics." SAE Paper 920582, 1992.
- [3] Takano, S. and M. Nagai. "Dynamics Control of Large Vehicles for Rollover Prevention." *IEEE Conf. on Vehicle Electronics* 2001: pp. 85-89.
- [4] Gertsch, J. and T. Shim. "Insightful Representations of Roll Plane Model Stability Limits." SAE Paper 2006-01-1284, 2006.
- [5] Hac, A. "Rollover Stability Index Including Effects of Suspension Design." SAE Paper 2002-01-0965, 2002.
- [6] Chen, B.-C. and H. Peng. "A Real-Time Rollover Threat Index for Sports Utility Vehicles." *Proc. of the American Control Conference* 1999: pp. 1233-37.

- [7] Preston-Thomas, J. and J.H.F. Woodrooffe. "A Feasibility Study of a Rollover Warning Device for Heavy Trucks." National Research Council of Canada Technical Report TR-VDL-005.
- [8] Hyun, D. and R. Langari. "Modeling to Predict Rollover Threat of Tractor-Semitrailers." *Vehicle System Dynamics* 39 (2003): pp. 401-14.
- [9] Heydinger, G.J. and J.G. Howe. "Analysis of Vehicle Response Data Measured During Severe Maneuvers." SAE Paper 2000-01-1644, 2000.
- [10] Dahlberg, E. "A Method Determining the Dynamic Rollover Threshold of Commercial Vehicles." SAE Paper 2000-01-3492, 2000.
- [11] Johansson, B. and M. Gäfvert. "Untripped SUV Rollover Detection and Prevention." *IEEE Conf. on Decision and Control* (2004): pp. 5461-66.
- [12] Dixon, J.C. *Tires, Suspension and Handling*. 2nd ed. Warrendale, PA: Society of Automotive Engineers, Inc., 1996.
- [13] Hac, A. "Rollover Stability Index Including Effects of Suspension Design." SAE Paper 2002-01-0965, 2000.
- [14] Gillespie, T. *Fundamentals of Vehicle Dynamics*. Warrendale, PA: Society of Automotive Engineers, Inc., 1992.
- [15] Hac, A., T. Brown, and J. Martens. "Detection of Vehicle Rollover." SAE Paper 2004-01-1757, 2004.
- [16] Dixon, J.C. "The Roll-Centre Concept in Vehicle Handling Dynamics." *Proc. Inst. Mechanical Engineers* 201 (1987): pp. 69-78.
- [17] Mitchell, W.C. "Asymmetric Roll Centers." SAE Paper 983085, 1998.
- [18] Vahidi, A., A. Stefanopoulou, and H. Peng. "Experiments for Online Estimation of Heavy Vehicle's Mass and Time-Varying Road Grade." *Int. Mechanical Engineering Congress and Exposition* (2003): 2003-42807.